

Material anisotropy unveiled by random scattering of surface acoustic waves

Vincent Laude,^{1,a)} Kimmo Kokkonen,² Sarah Benchabane,¹ and Matti Kaivola²

¹Institut FEMTO-ST, Université de Franche-Comté and CNRS, 32 Avenue de l'Observatoire, F-25044 Besançon, France

²Department of Applied Physics, Aalto University, Tietotie 3, 02150 Espoo, Finland

(Received 10 December 2010; accepted 21 January 2011; published online 11 February 2011)

We consider launching a monochromatic surface acoustic wave packet on a large set of random scatterers. The interference of the multiple scattered waves creates a random pattern of ripples on the crystal surface that is recorded by optical interferometry. The Fourier transform of the amplitude and phase data of the measured wave field unveils the complete slowness curve, i.e., the wave-vector as a function of the propagation angle. A simple acoustic speckle model is proposed to explain this observation. © 2011 American Institute of Physics. [doi:10.1063/1.3554424]

The structural anisotropy of crystalline solids directly influences the velocity of acoustic waves or phonons. Conversely, the measurement of the velocity as a function of the angle of propagation allows one to evaluate the elasticity tensor of the material. The observation of waves propagating at the surface of solids has been performed by various means. Matsuda *et al.* performed pump-probe experiments in which they could observe the ripples originating from a punctual excitation of surface acoustic waves (SAWs).¹ In these time-domain experiments, they demonstrated that a few wavelengths away from the source, the phase front follows the shape of the surface wave, i.e., the locus of the group velocity as a function of the propagation angle, $v_g(\theta)$. Alternatively, frequency-domain experiments can be conducted at a fixed wavelength to evaluate the slowness curve, i.e., the inverse of the phase velocity of a plane wave as a function of the phase angle, $s(\varphi)$. There is a simple and direct relation between the slowness curve and the wave surface, $v_g(\theta)=[s(\varphi)\cos(\psi)]^{-1}$, with ψ as the beam-steering angle and $\theta=\varphi+\psi$.^{2,3} Accurate knowledge of the slowness curve is needed in the design of SAW devices, as illustrated by tailored interdigital transducers (IDTs) that can focus a SAW beam⁴ or even create a subwavelength acoustic source.⁵ Wickramasinghe and Ash⁶ showed that SAW slowness curves can be measured using a phase sensitive laser probe. Indeed, given the wave field distribution obtained from a SAW transducer emitting within some angular range, they obtained the corresponding portion of the slowness curve by a one-dimensional Fourier transform (FT) of two line scans separated by a given distance. Robbins and Rudd⁷ performed a similar experiment by using a scanning laser acoustic microscope. They observed that the waves scattered from the edges of their sample contribute to the measurement, although very faintly. Later on, a scanning acoustic force microscope was also used to observe the phase velocity of surface waves.⁸

In this letter, we consider obtaining the full slowness curve without prior knowledge of the elastic constants. Whereas the previously described methods resolve an angular range limited by the emission of the transducer, we consider the random interference of surface waves coming from

all possible angles of incidence. This interference forms an acoustic speckle field that contains all the necessary information for extracting the slowness curve via a Fourier transform if the coherence of the surface waves is properly captured. To this end, we use a scanning heterodyne optical probe⁹ that records both the phase and absolute amplitude of the acoustic speckle field.

In our experiment, we selected the Y-cut of lithium niobate (LiNbO₃) as the anisotropic substrate material. The experiment is depicted in Fig. 1. The IDTs have 50 finger pairs, a pitch of 8 μm , and an aperture of 500 μm . The surface of the scan area is metallized with 150 nm of aluminum. Note that the same design would operate on any piezoelectric substrate whatever the crystalline orientation and with or without the central metallization. The frequency of the monochromatic SAW is tuned to 223 MHz (near the IDT resonance) using a signal generator. The collimated SAW beams are directed toward regions containing many random

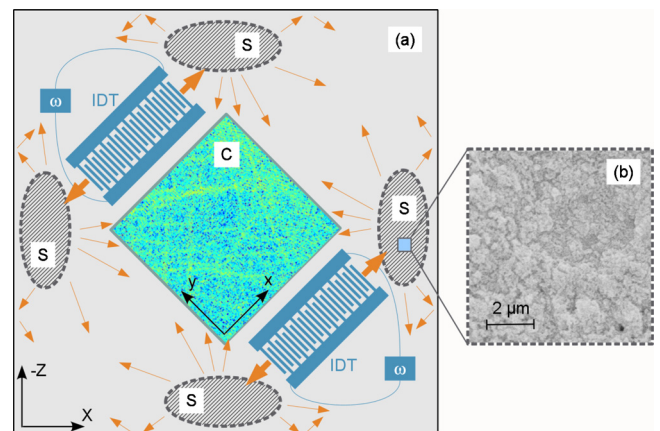


FIG. 1. (Color online) Schematic presentation of the experiment proposed to obtain the slowness curve from random SAW scattering (not to scale). (a) Two identical IDTs generate SAWs at angular frequency ω , which propagate toward regions containing a large number of random scatterers (S). The scattered SAWs generate a random wave field, or speckle, that is captured in the central area (c) using a scanning heterodyne optical probe. The amplitude of one such scan is shown in the central area for illustration. The set of axes with capital letters is for the crystallographic directions while the other set of axes is for the measurement coordinate-system. (b) A scanning electron microscope view inside one of the regions with random scatterers (S) is shown.

^{a)}Electronic mail: vincent.laude@femto-st.fr.

scatterers. These regions are created by repetitively scanning a femtosecond laser beam over the crystal surface along many different directions. The complex interplay of material ablation and redeposition then creates scattering structures that are irregular in shape, with lateral dimensions much smaller than the incident acoustic wavelength. Each scatterer is expected to convert part of the incoming SAW beam to annular SAWs.¹⁰ The scattered surface waves travel on the surface and interfere, creating an acoustic speckle similar to the laser speckle observed on a screen where a continuous-wave laser beam is diffused. The coherence time of the signal delivered by the frequency generator is much longer than 1 s and even though some phase noise is introduced by the experimental set-up, we infer that the coherence time of the SAW is larger than 1 s. Considering an average velocity of 3500 m/s, the scattered SAW can then propagate over distances larger than 3500 m and still interfere with subsequent incoming SAWs. Given that the sample size is a few centimeters, the acoustic speckle remains perfectly coherent even after many scattering events.

The intensity and the phase of the acoustic speckle are random quantities originating from the interference of the scattered waves. In the experiment depicted in Fig. 1, the acoustic speckle field is sampled over a certain area away from all sources, i.e., both away from the IDTs and the scatterers. The scanning heterodyne optical probe is sensitive to the vertical displacement of the surface.^{9,11} The amplitude and phase of the measured speckle field are shown in Fig. 2, together with the FT result. It can be seen that the FT is also a random quantity but that its distribution concentrates mostly along a closed curve in Fourier (wave-vector) space. This closed curve is the slowness curve for SAWs propagating on the crystal surface. This observation is confirmed by comparing the measured closed curve, Fig. 2(c), with the slowness curve computed¹⁰ using the material constants in Ref. 12, Fig. 2(d).

It can also be observed that the interior of the measured slowness curve is filled with a random background, while its exterior shows no wave contributions. We attribute this to the waves that are scattered to the bulk of the substrate. Since these are trapped between the two surfaces of the crystal plate, they can propagate at any angle. Their wave-vector in the surface plane is, however, limited to that of the slowest bulk acoustic wave as they are constrained to the sound cone. The calculated projection of the sound cone is depicted in Fig. 2(d) as a gray area for comparison with the experimental result. Furthermore, it can be noted that the experiment also reproduces the ‘forbidden’ regions between the SAW slowness curve and the projected sound cone. This is seen in the experiment as the blue area between the filled interior and the slowness curve.

We now formulate a simple model for the formation of the SAW speckle and of its Fourier transform. Bulk contributions are neglected in this analysis, which is limited to SAWs in the far-field of the sources. At any observation point \mathbf{r} , a large number of scattered waves are received. We assume that the scatterers can be regarded as point sources, or equivalently, that their size is much smaller than the SAW wavelength at frequency ω . We formally write this superposition as

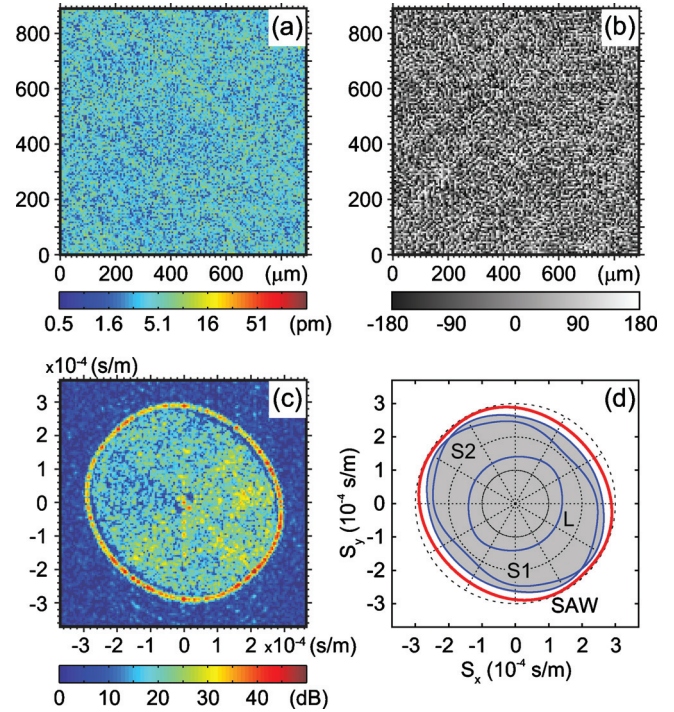


FIG. 2. (Color) Experimental measurement of the SAW speckle at 223 MHz and comparison to the simulated slowness curve. The measured absolute amplitude and phase (in degrees) of the surface vibration field are shown in (a) and (b), respectively. The Fourier transform of the measured wave field in (c) shows the wave content as a function of slowness (or inverse phase velocity). The SAW slowness curve is seen as the continuous outer boundary and waves scattered into the bulk as the filled interior disk. The calculated dispersion relation is displayed in (d), with the computed SAW slowness curve shown as a solid red line and the projection of the sound cone for bulk waves shown as a gray region. Bulk waves propagating in the plane of the surface are identified and labeled as S1, S2, and L for the two shear and the longitudinal waves, respectively.

$$u(\mathbf{r}) = \sum_n A_n G_\omega(\mathbf{r} - \mathbf{r}_n). \quad (1)$$

In this equation, u is the vertical displacement, A_n is a random variable (the oscillation amplitude of the n th scatterer), and G_ω is a Green's function giving the field scattered by a point scatterer.¹⁰ It is important to note that we assume that the Green's function is independent of the particular scatterer considered. The statistical properties of A_n need not to be precisely known. However, it can be assumed for simplicity that they correspond to white noise with the properties $\langle A_n \rangle = 0$ and $\langle A_n^* A_m \rangle = \sqrt{I_n} \sqrt{I_m} \delta_{nm}$, where the scatterers can have unequal amplitude variance. It is useful to consider the following spectral representation of the Green's function

$$G_\omega(r, \theta) = \int_0^{+\infty} \frac{kdk}{4\pi^2} \int_0^{2\pi} d\varphi \tilde{G}_\omega(k, \varphi) e^{-ikr \cos(\theta-\varphi)}. \quad (2)$$

In the far-field of a scatterer, the Green's function is dominated by the SAW contribution, which possesses a singular kernel lying on the slowness curve so that the spectral Green's function can be approximated by the single-pole formula¹⁰

$$\tilde{G}_\omega(k, \varphi) = \frac{a(\varphi)}{k - \omega s(\varphi)}. \quad (3)$$

The (unbounded) Fourier transform of Eq. (1) is

$$\tilde{u}(\mathbf{k}) = \left(\sum_n A_n e^{i\mathbf{k}\cdot\mathbf{r}_n} \right) \tilde{G}_\omega(\mathbf{k}). \quad (4)$$

From this expression, we observe that the FT of the vertical displacement field is the product of a random function and of the singular spectral Green's function. Since the FT of white noise is also white noise, the FT of the speckle appears as an image of random bright and dark spots. The singularity of the spectral Green's function enhances very locally the FT of the speckle and hence makes the slowness curve visible.

The previous analysis would result in speckle grains having a vanishing size. This idealization is a consequence of our assumption of an infinite number of random sources in Eq. (1) and their pointlike extent. There are at least two limiting dimensions in our experiment. First, the step size of the scan limits the maximum spatial frequency. In practice, it is sufficient to have a few samples per wavelength to satisfy the Nyquist criterion. Second, the lateral size of the scan, Δx , limits the spatial frequency resolution. The speckle grain size can roughly be estimated to be inversely proportional to the size of the scanning window. Denoting this window $W(\mathbf{r})$, Eq. (1) can be rewritten as

$$u_W(\mathbf{r}) = \sum_n A_n G_\omega(\mathbf{r} - \mathbf{r}_n) W(\mathbf{r}). \quad (5)$$

The spatial Fourier transform of this expression is

$$\tilde{u}_W(\mathbf{k}) = \int \frac{d\mathbf{k}'}{4\pi^2} \tilde{u}(\mathbf{k}') \tilde{W}(\mathbf{k} - \mathbf{k}'). \quad (6)$$

In the experiment, the scanning area is bounded and the Fourier transform of the scanned amplitude and phase field is thus the convolution of a speckle grain function times the FT of the unbounded acoustic speckle field. The speckle grain function is the Fourier transform of the window function. The relative spatial frequency resolution can be roughly estimated as $\lambda/\Delta x$. In the experiment presented here, this relative resolution is around 2%. This number can be improved by using a larger scan area, of course, at the expense of a

longer scan time. Furthermore, *a priori* knowledge of the properties of the SAW slowness curve (for instance, that it is a continuous and periodic function of the angle) could be incorporated in the estimation algorithm.

As a conclusion, we have shown that the slowness curve for surface acoustic waves, a direct measure of the anisotropy of a solid material, can be recovered by recording the acoustic speckle originating from random scattering. The measurement of the phase of the acoustic speckle field, in addition to its amplitude, is essential in this process. We have proposed a simple model for the formation of the acoustic speckle, stressing the importance of the singularity of the spectral Green's function along the slowness curve. The method could be used, for example, to estimate the elastic constants of anisotropic media.

The authors gratefully acknowledge the assistance of Roland Salut during the femtosecond laser milling of the random scatterers.

¹D. M. Profunser, O. B. Wright, and O. Matsuda, *Phys. Rev. Lett.* **97**, 055502 (2006).

²B. A. Auld, *Acoustic Fields and Waves in Solids* (Wiley, New York, 1973).

³D. Royer and E. Dieulesaint, *Elastic Waves in Solids* (Wiley, New York, 1999).

⁴M. M. de Lima, F. Alsina, W. Seidel, and P. V. Santos, *J. Appl. Phys.* **94**, 7848 (2003).

⁵V. Laude, D. Gérard, N. Khelifaoui, C. F. Jerez-Hanckes, S. Benchabane, and A. Khelif, *Appl. Phys. Lett.* **92**, 094104 (2008).

⁶H. K. Wickramasinghe and E. A. Ash, *Proc.-IEEE Ultrason. Symp.* **1975**, 496.

⁷W. P. Robbins and E. P. Rudd, *J. Appl. Phys.* **64**, 1040 (1988).

⁸T. Hesjedal and G. Behme, *Appl. Phys. Lett.* **79**, 1054 (2001).

⁹K. Kokkonen and M. Kaivola, *Appl. Phys. Lett.* **92**, 063502 (2008).

¹⁰V. Laude, C. F. Jerez-Hanckes, and S. Ballandras, *IEEE Trans. Ultrason. Ferroelectr. Freq. Control* **53**, 420 (2006).

¹¹K. Kokkonen, M. Kaivola, S. Benchabane, A. Khelif, and V. Laude, *Appl. Phys. Lett.* **91**, 083517 (2007).

¹²G. Kovacs, M. Anhorn, H. E. Engan, G. Visintini, and C. C. W. Ruppel, *Proc.-IEEE Ultrason. Symp.* **1**, 435 (1990).